



Joint ESS ILL User Meeting

5-7 October 2022

Lund, Sweden

Neutron scattering studies on CO₂ confined in nanoporous materials: Applications to CO₂ sequestration and oil recovery

K.L. Stefanopoulos, Ph.D.

Institute of Nanoscience and Nanotechnology

National Center for Scientific Research "Demokritos"

Athens-Greece



ΔΗΜΟΚΡΙΤΟΣ



National Centre for Scientific Research “DEMOKRITOS”

Aghia Paraskevi - Athens - Greece



5 Research Institutes
Personnel: ~1000

- **Nanoscience & Nanotechnology**
- **Informatics & Telecommunications**
- **Biosciences & Applications**
- **Nuclear & Radiological Sciences, Technology, Energy & Safety**
- **Nuclear & Particle Physics**

Contents:

- **CO₂ confined in model pore systems (MCM-41, SBA-15)**
- **CO₂ confined in complex pore systems (limestone)**

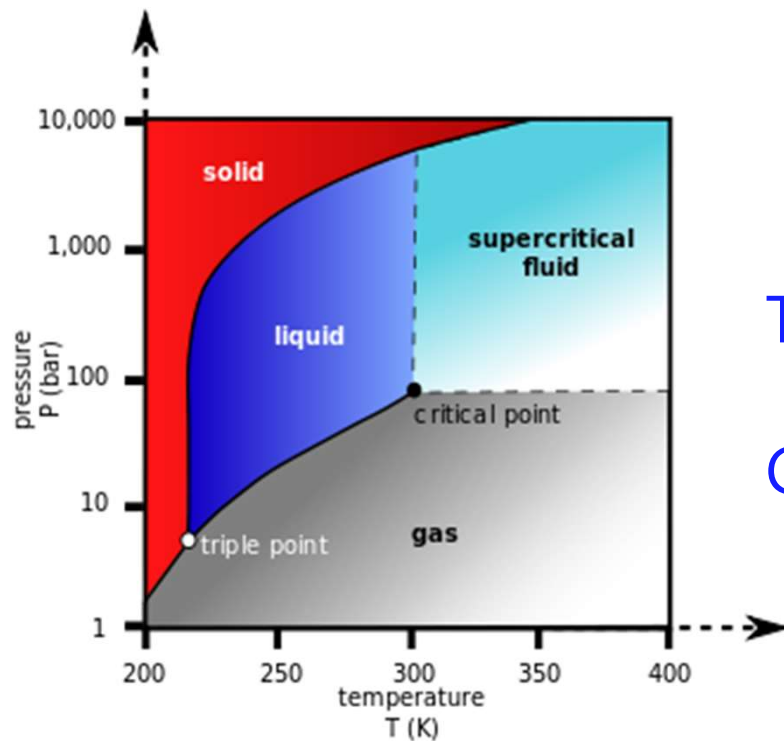
Why carbon dioxide?

Simple molecule with linear shape

Strong quadrupole moment - Orientational effects

sc-CO₂ solvent, Enhanced Oil Recovery (EOR) , Geological sequestration

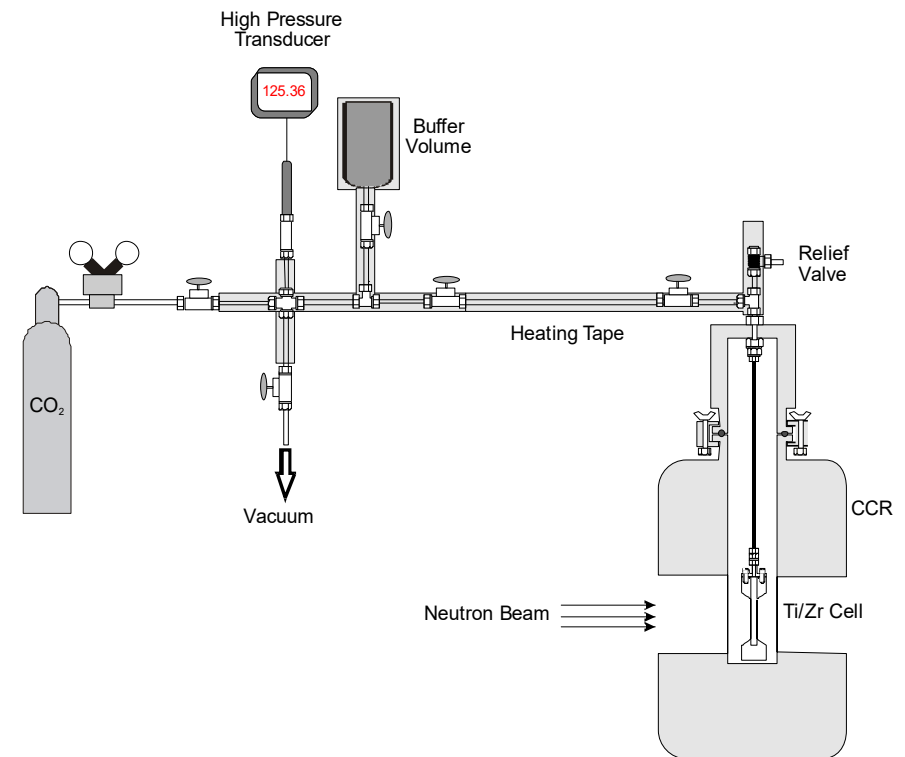
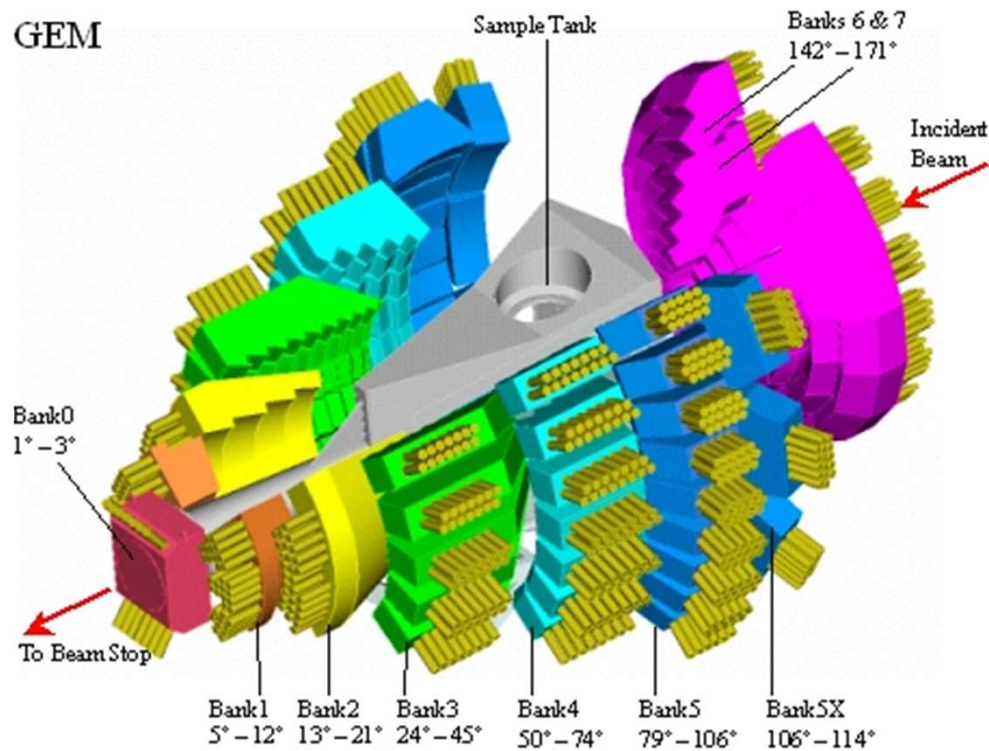
When pore-confined, the finite volume geometry and the surface-fluid interactions can alter its properties and influence its phase behaviour



Triple point: $T_3=216.6$ K, $P_3=5.2$ bar

Critical point: $T_c=304.1$ K, $P_c=73.8$ bar

Performing in situ neutron diffraction measurements upon
CO₂ adsorption along an isotherm at 253 K in MCM-41



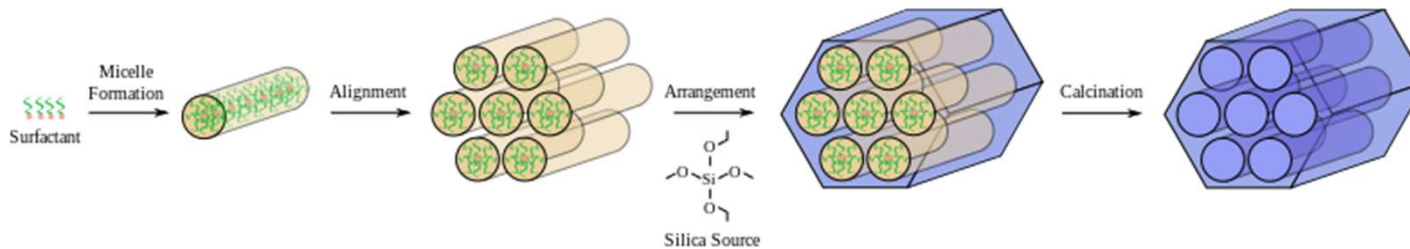
General materials powder diffraction (GEM, ISIS)

GEM detector array has 7270 elements,

8 detector banks

Scattering angle range from 1° to 171°

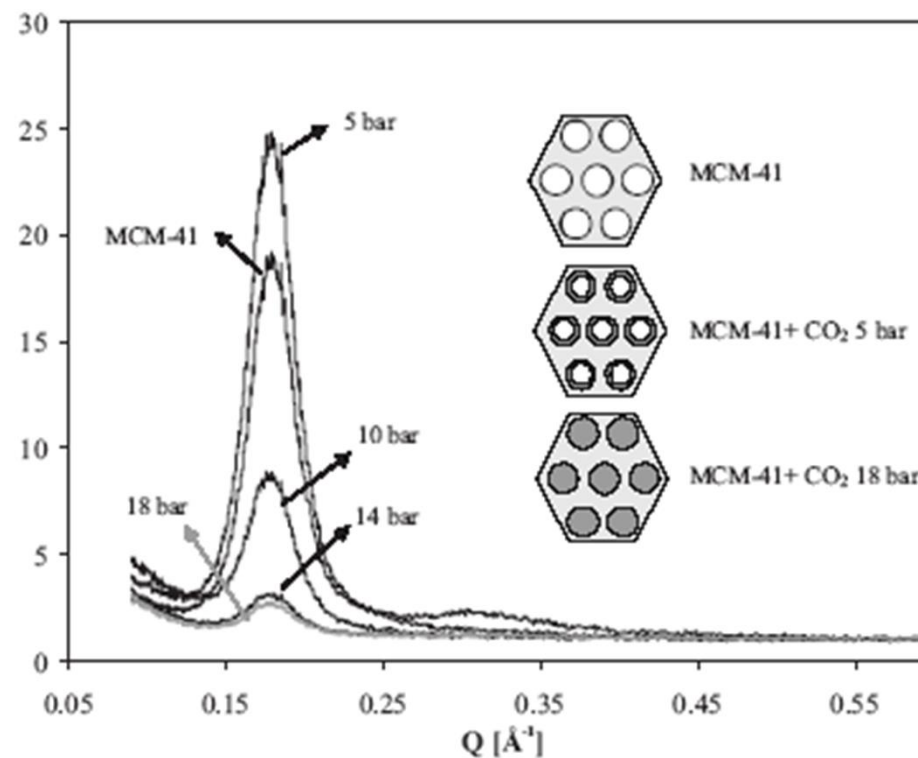
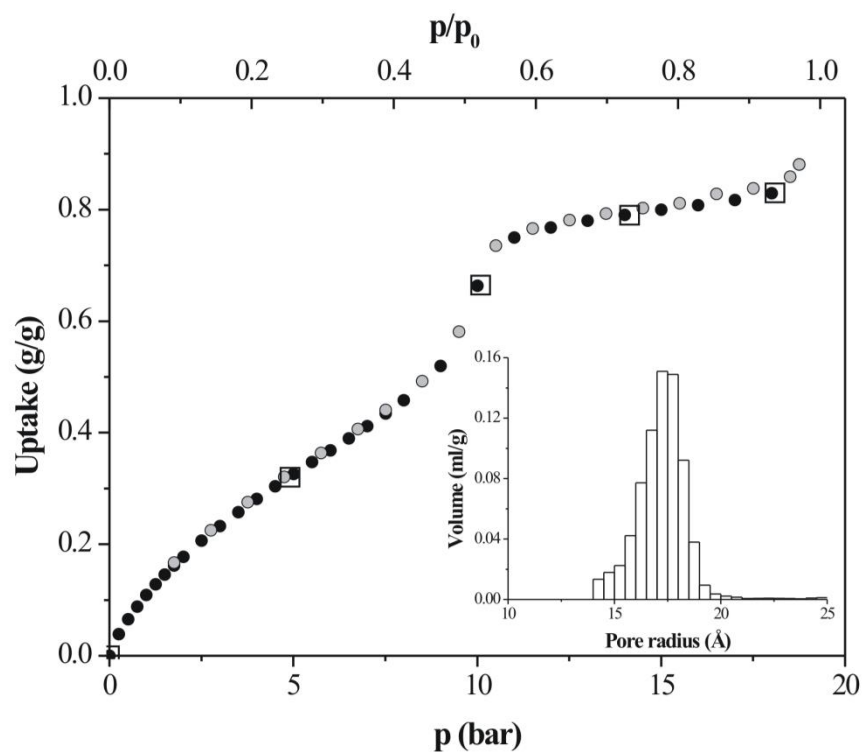
Q-range: 0.02-40 \AA^{-1} $\Delta Q/Q=0.35\%$ (bank 7)



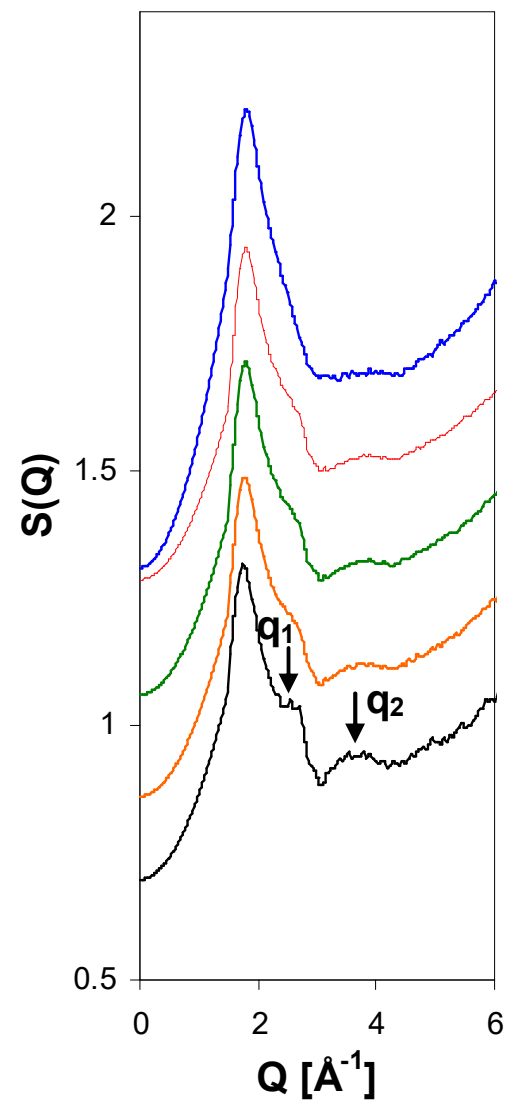
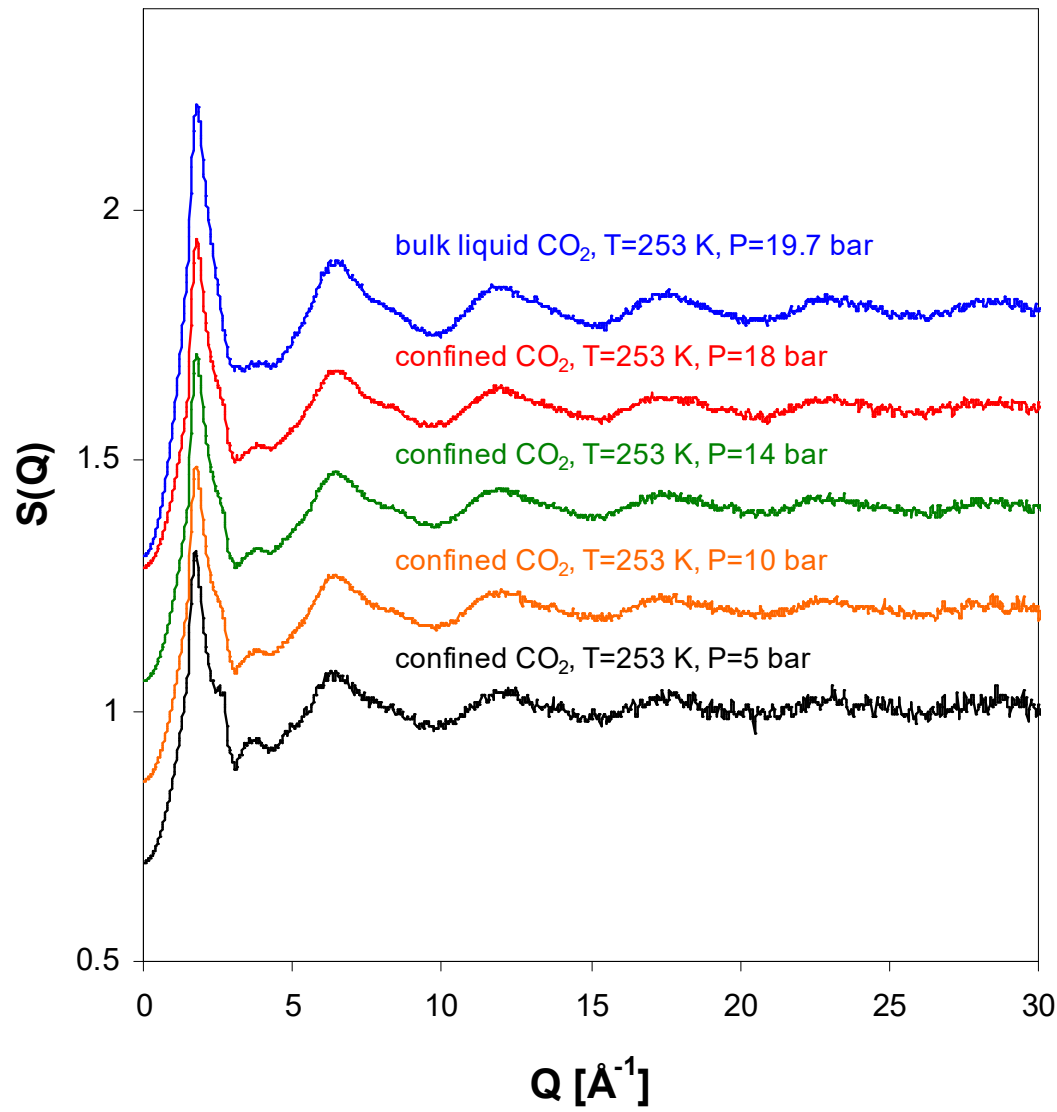
| Sample | S_{BET} (m ² /g) | V_p (cm ³ /g) | D_{BJH} (Å) | D_{NLDFT} (Å) |
|--------|---|-------------------------------|-------------------------|---------------------------|
| MCM 41 | 1200 | 0.86 | 23 | 35 |

2D hexagonally ordered array of cylindrical pores ($p6mm$ space group)

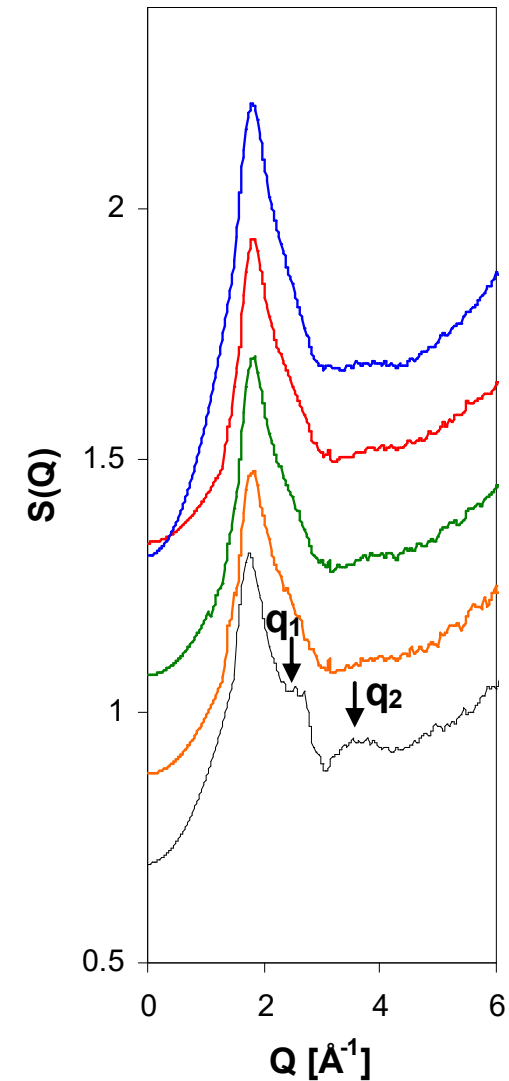
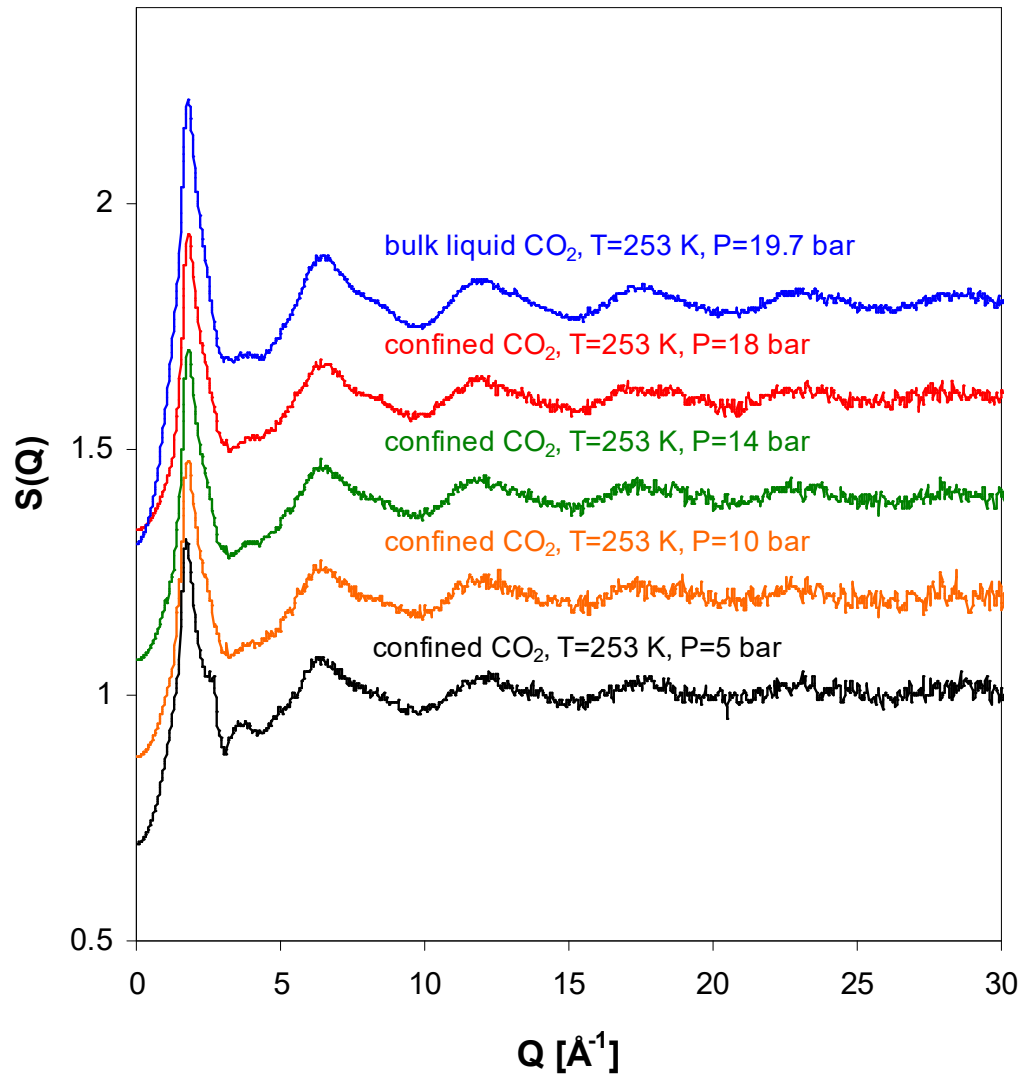
$T=253$ K, $5 \leq P \leq 18$ bar



| | |
|---|--|
| differential cross section | $\frac{d\sigma}{d\Omega} = I^S(Q) + i(Q)$ |
| self-scattering | $I^S(Q)$ |
| distinct scattering | $i(Q)$ |
| structure factor | $S(Q) = \frac{i(Q)}{\sum_{i=1}^n c_i b_i^2} + 1$ |
| for a molecular liquid | $S_M(Q) = f_1(Q) + D_M(Q) = f_1(Q) + \frac{4\pi}{Q} \rho_M \int [g_L(r) - 1] r \sin(Qr) dr$ |
| intramolecular form factor | $f_1(Q)$ |
| intermolecular contribution | $D_M(Q)$ |
| liquid density | ρ_M |
| intermolecular pair correlation function | $g_L(r)$ |
| differential correlation function | $D(r) = 4\pi\rho_M [g_L(r) - 1] = \frac{2}{\pi} \int_0^\infty Q [S_M(Q) - 1] M(Q) \sin(Qr) dQ$ |
| Lorch function | $M(Q)$ |
| for confined CO₂ | $S(Q) = S^{\text{CO}_2}(Q) + 2 \sqrt{\frac{X_{\text{SiO}_2}}{X_{\text{CO}_2}}} \frac{b_{\text{SiO}_2}}{b_{\text{CO}_2}} S^{\text{SiO}_2-\text{CO}_2}(Q)$ |
| total structure factor of CO ₂ | $S^{\text{CO}_2}(Q)$ |
| cross correlation term | $S^{\text{SiO}_2-\text{CO}_2}(Q)$ |

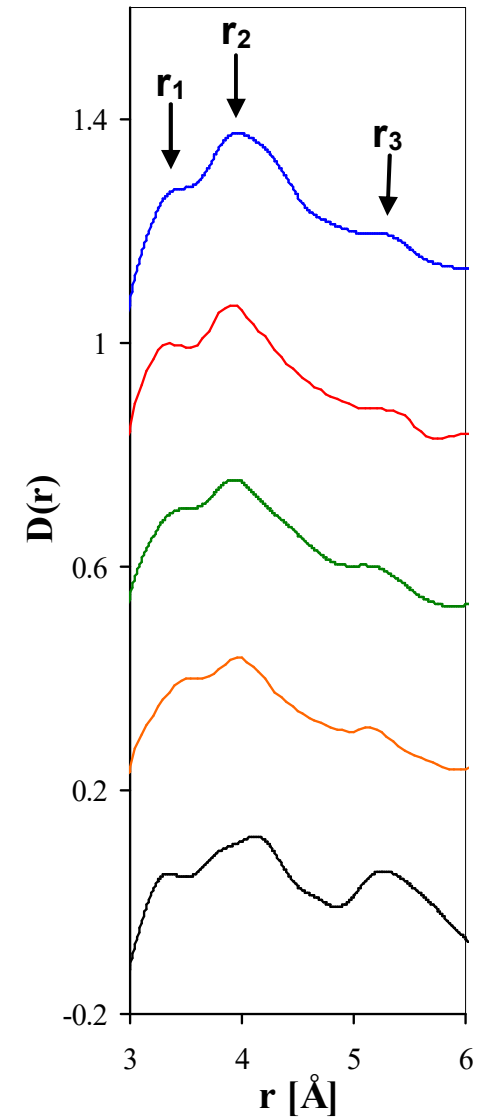
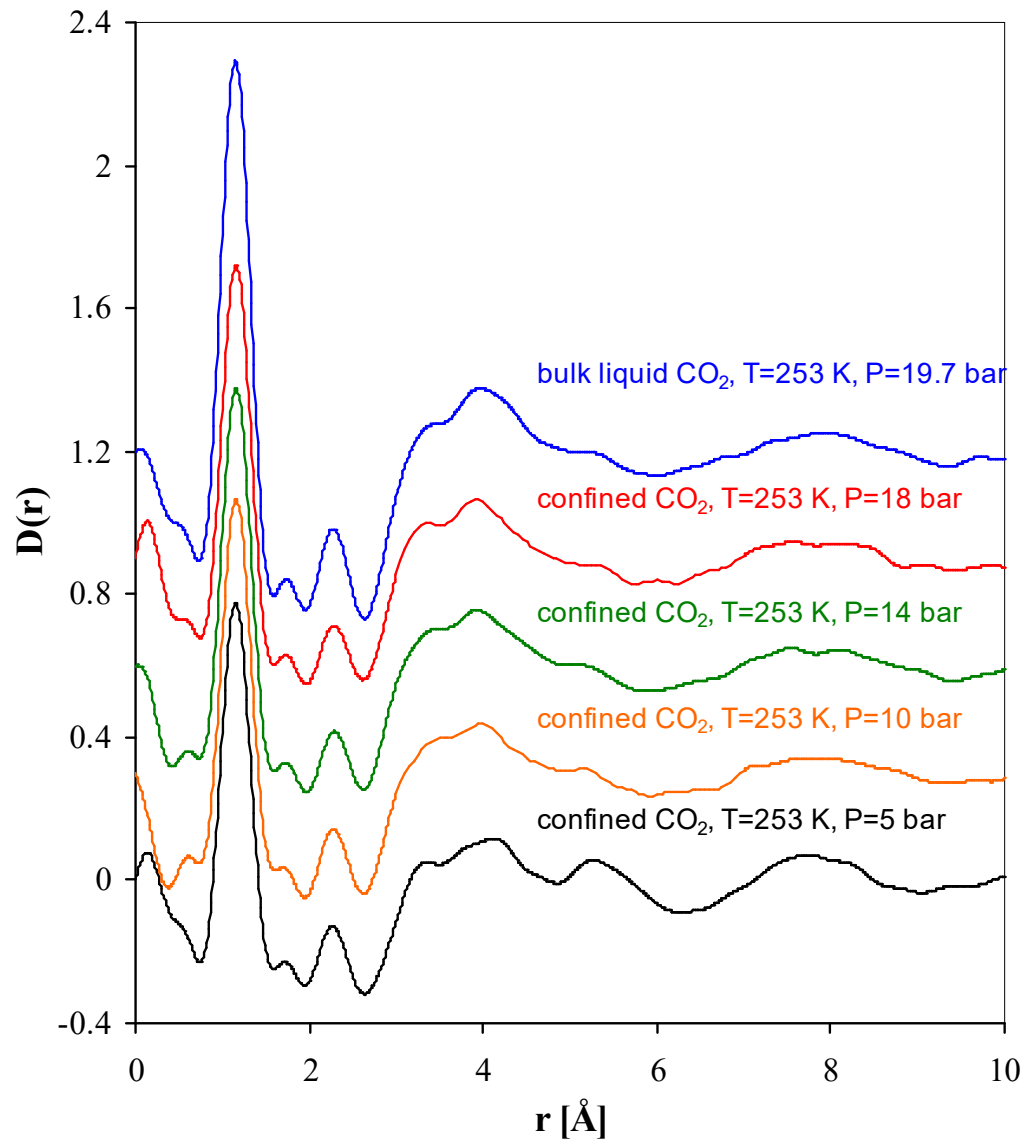


Total scattering structure factors for bulk liquid and confined CO₂



Total scattering structure factors for bulk liquid and confined CO₂

Minimization of the cross correlation term or elimination of the contribution of the monolayer structure



Differential correlation functions for bulk liquid and confined CO_2

Th.A. Steriotis, K.L. Stefanopoulos, F.K. Katsaros, R. Gläser, A.C. Hannon, J.D.F. Ramsay, **Phys. Rev. B**, 78 (2008) 115424

Summary

- **CO₂ adsorption with *in situ* neutron diffraction measurement on MCM-41 along an isotherm at $T=253$ K (GEM, ISIS).**
- **Selection of a diffractometer with a wide accessible Q range.**
- **The structure factors and the total differential correlation functions of confined CO₂ suggest that the confined fluid has at all studied thermodynamic states liquid-like properties, however several subtle differences, pointing to stronger orientational correlations inside the pores, were observed.**
- **Molecular simulation approaches coupled with experimental results would throw more light in the molecular arrangement under confinement.**

➤ **CO₂ confined in model pore systems (SBA-15)**

NIMROD

(Near and InterMediate Range-Order Diffractometer)

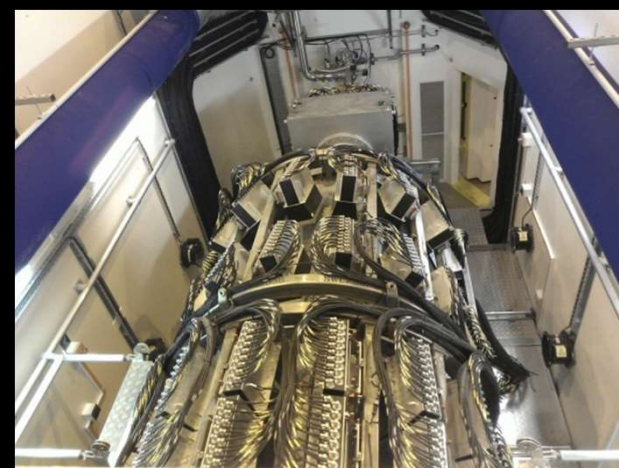
Measures Total Scattering and SANS:

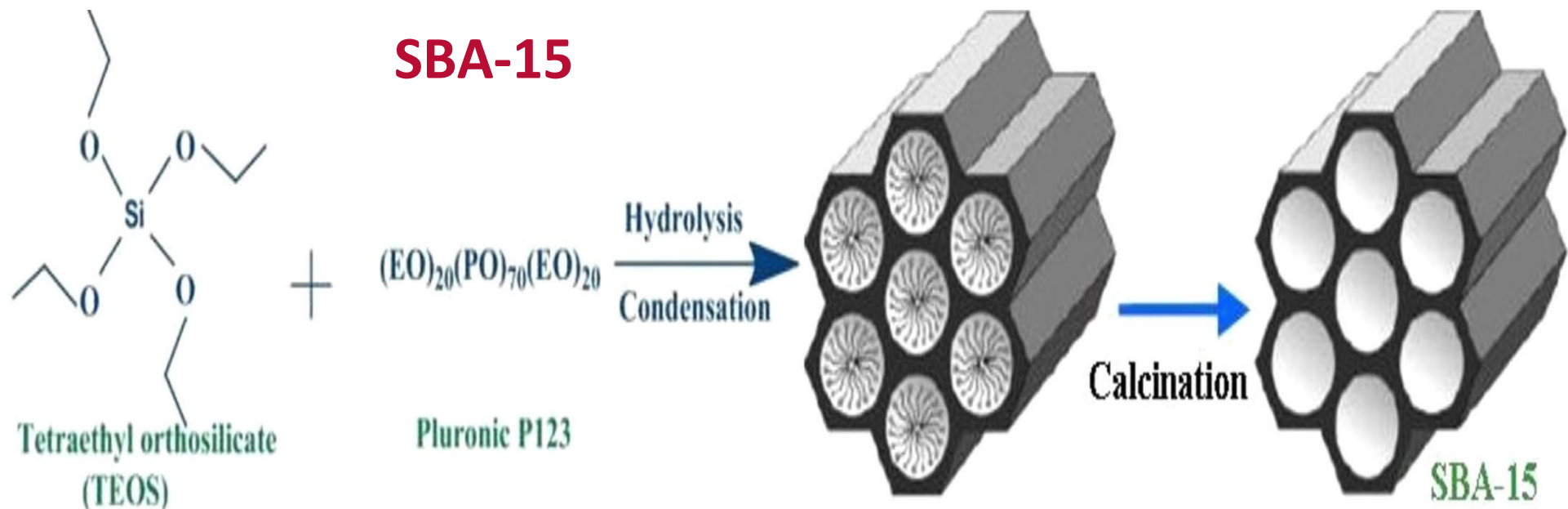
- Bragg scattering ($0.4 < \vartheta < 40^\circ$)
- Diffuse scattering ($0.1 < r < 300 \text{ \AA}$)
- **SANS ($0.01 < Q < 50 \text{ \AA}^{-1}$)**

Bragg scattering - crystalline components

Diffuse scattering - disordered materials

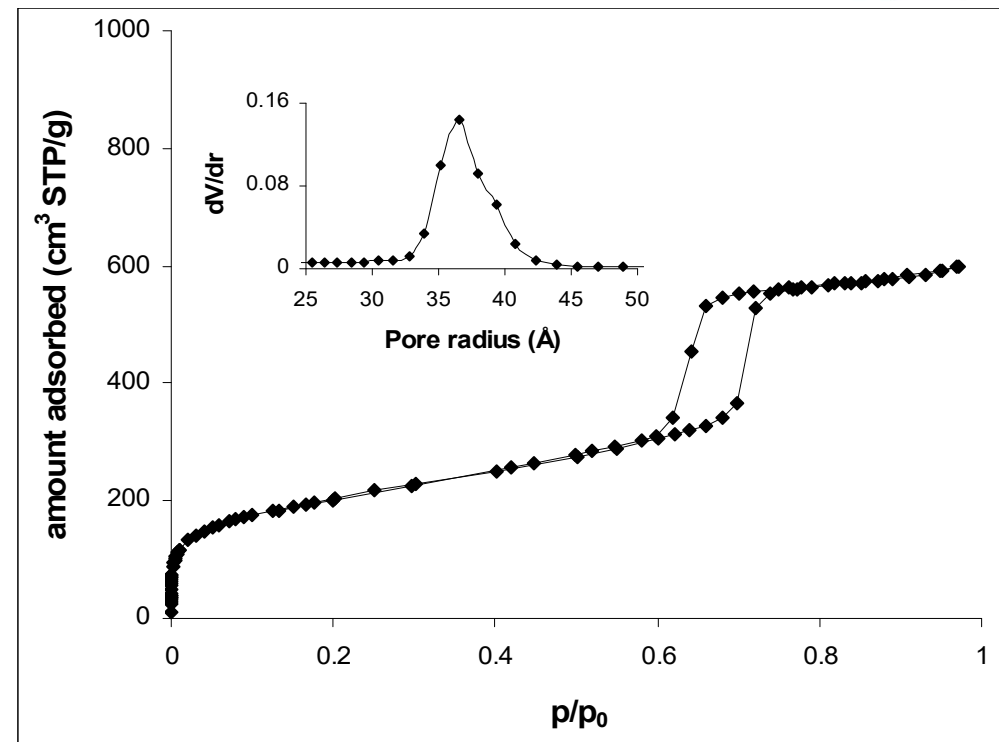
SANS – covers a part of small-angle region





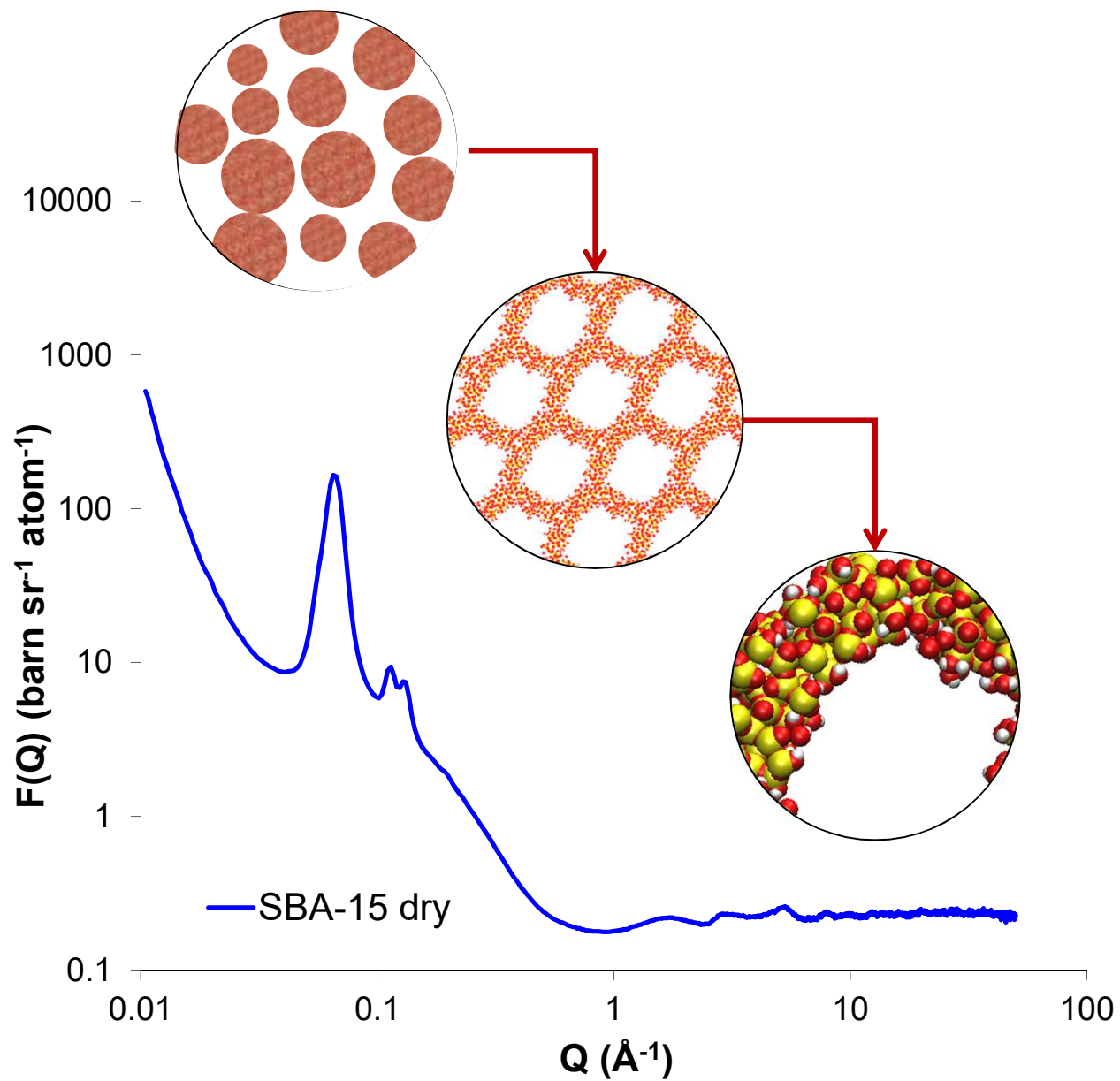
2D hexagonal array of cylindrical pores (p6mm space group)

| Sample | S_{BET} (m ² /g) | V_p (cm ³ /g) | D_{BJH} (Å) | D_{NLDFT} (Å) |
|--------|---|-------------------------------|-------------------------|---------------------------|
| SBA-15 | 700 | 0.93 | 56 | 74 |

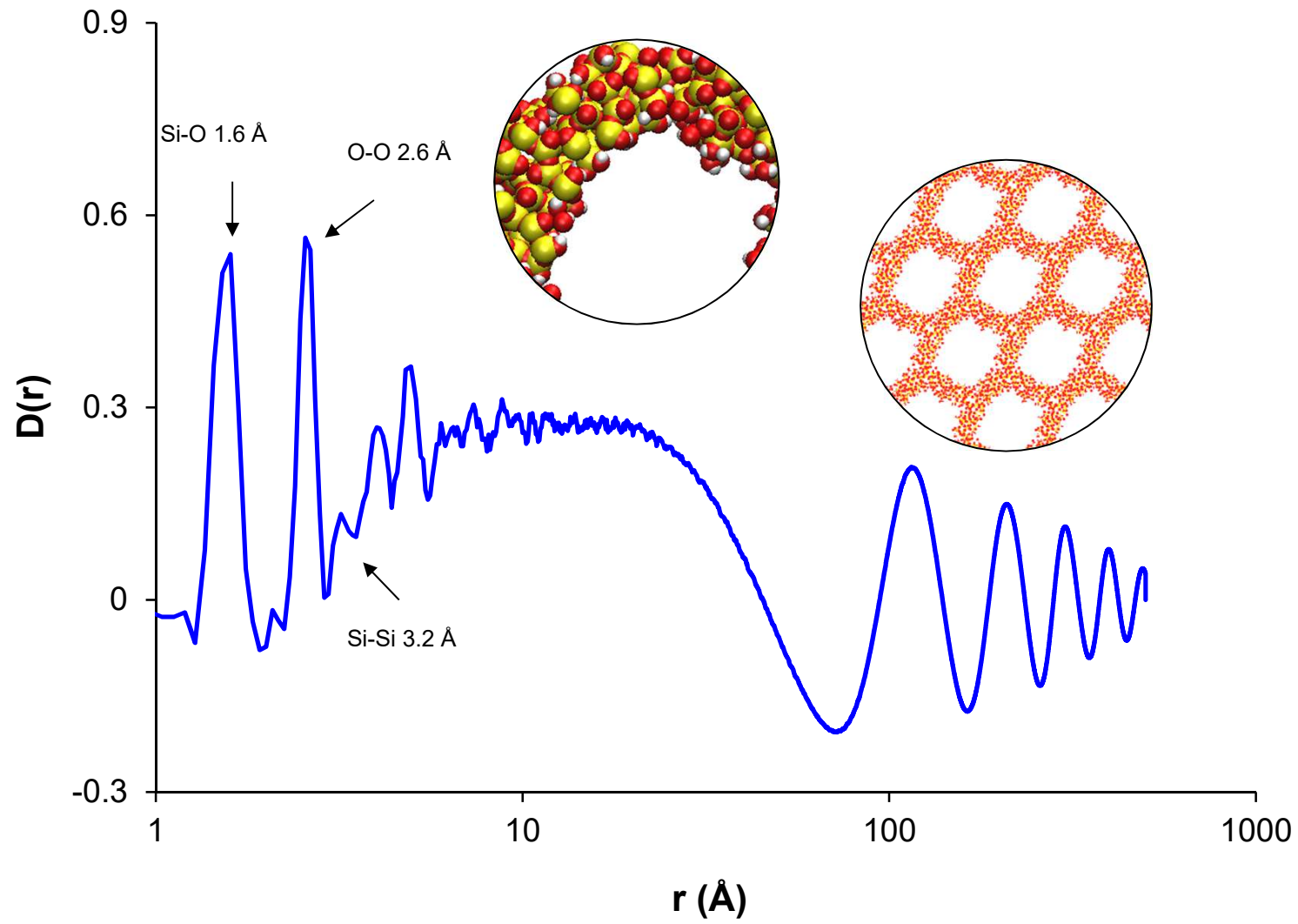


Nitrogen adsorption isotherm at 77 K

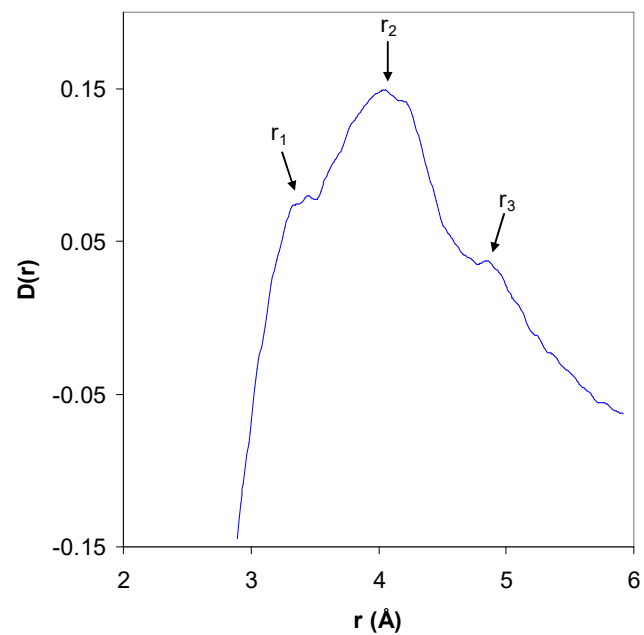
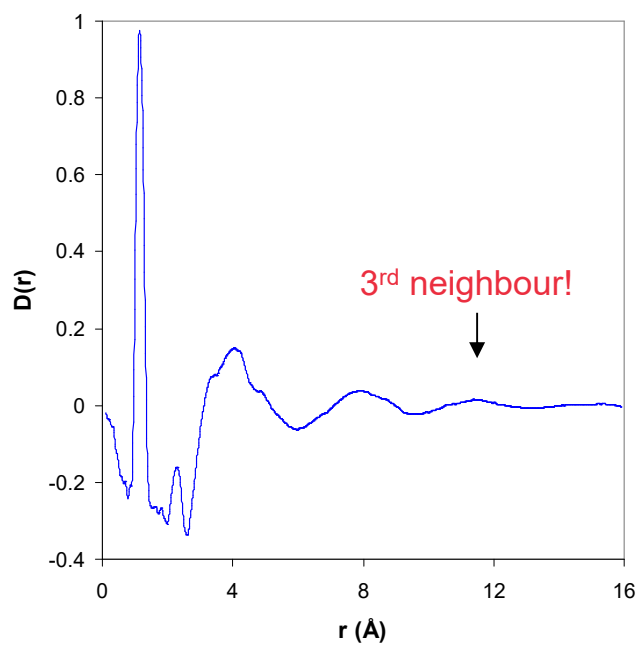
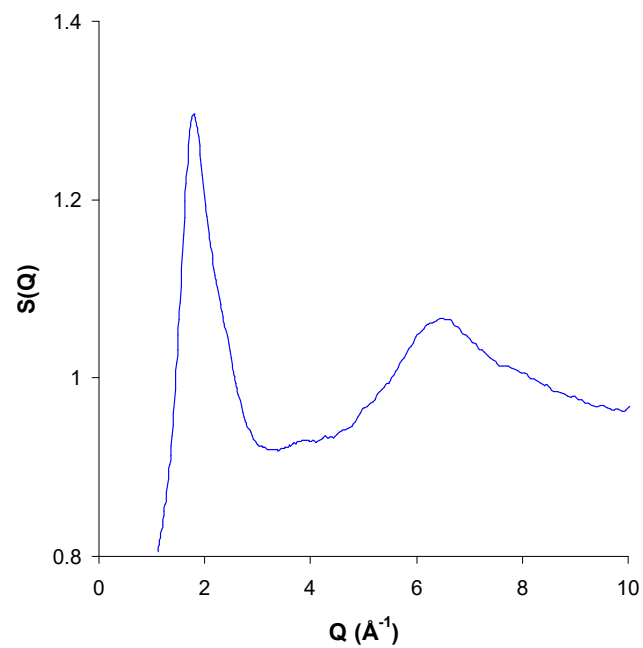
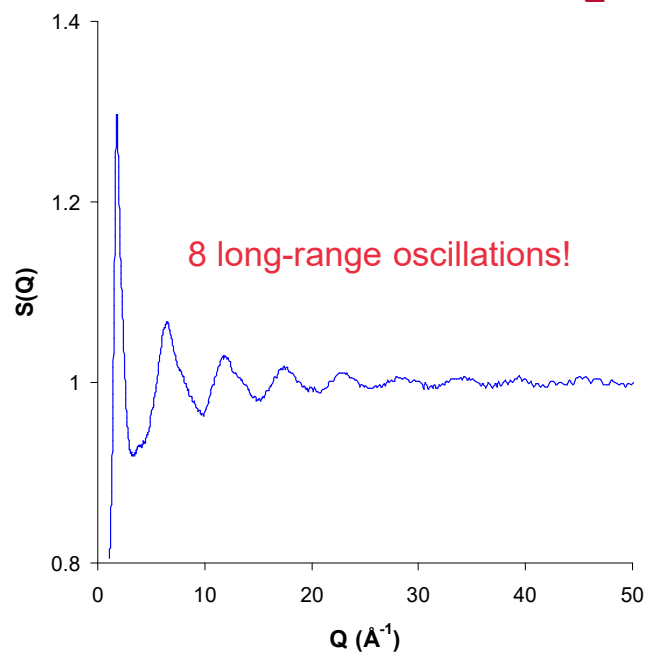
Differential cross section of SBA-15



Differential correlation function of SBA-15

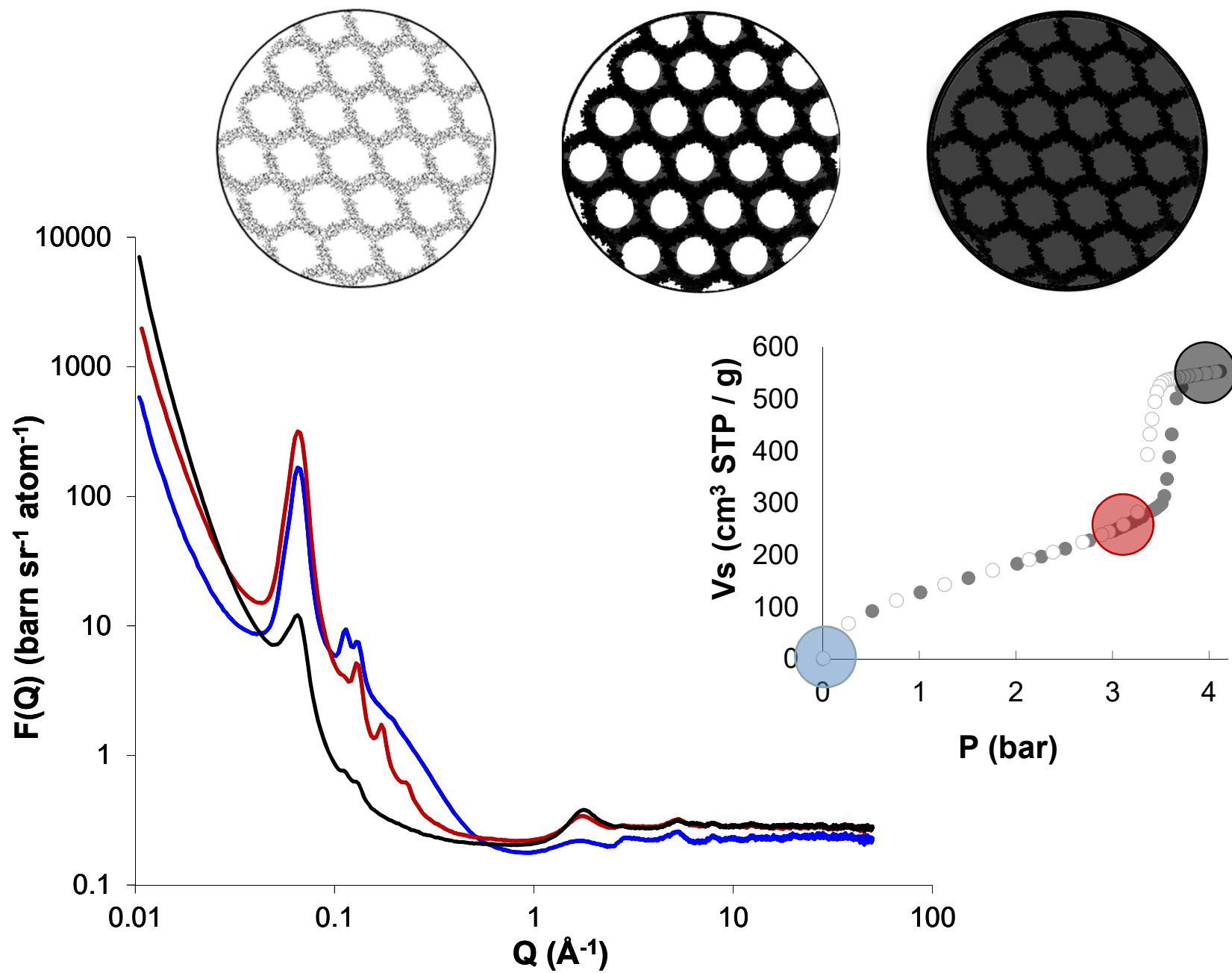


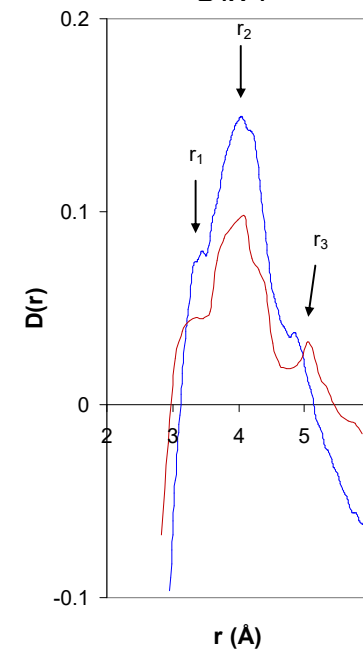
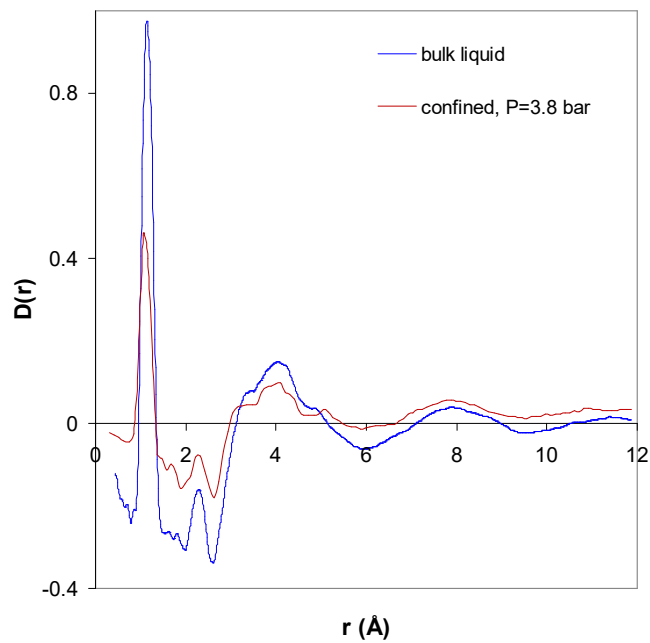
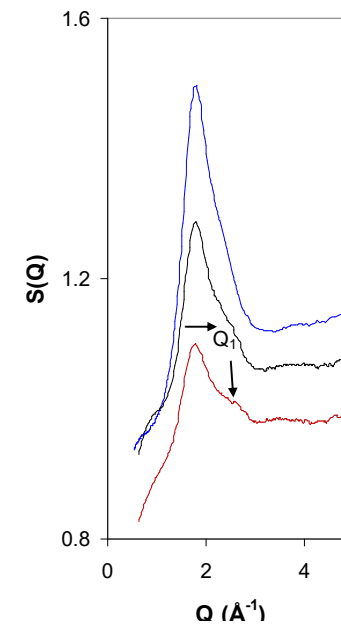
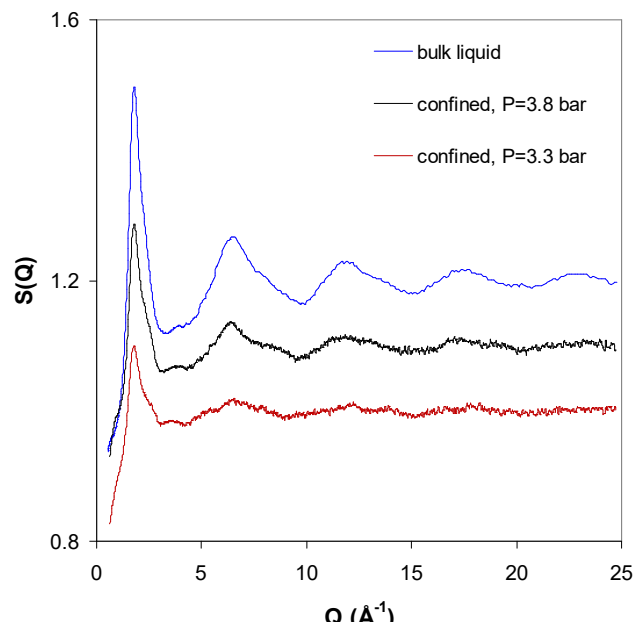
Bulk liquid CO₂: $T=230$ K, $P=12$ bar



Total scattering structure factor and differential correlation function for bulk liquid CO₂

CO₂ confined in SBA-15

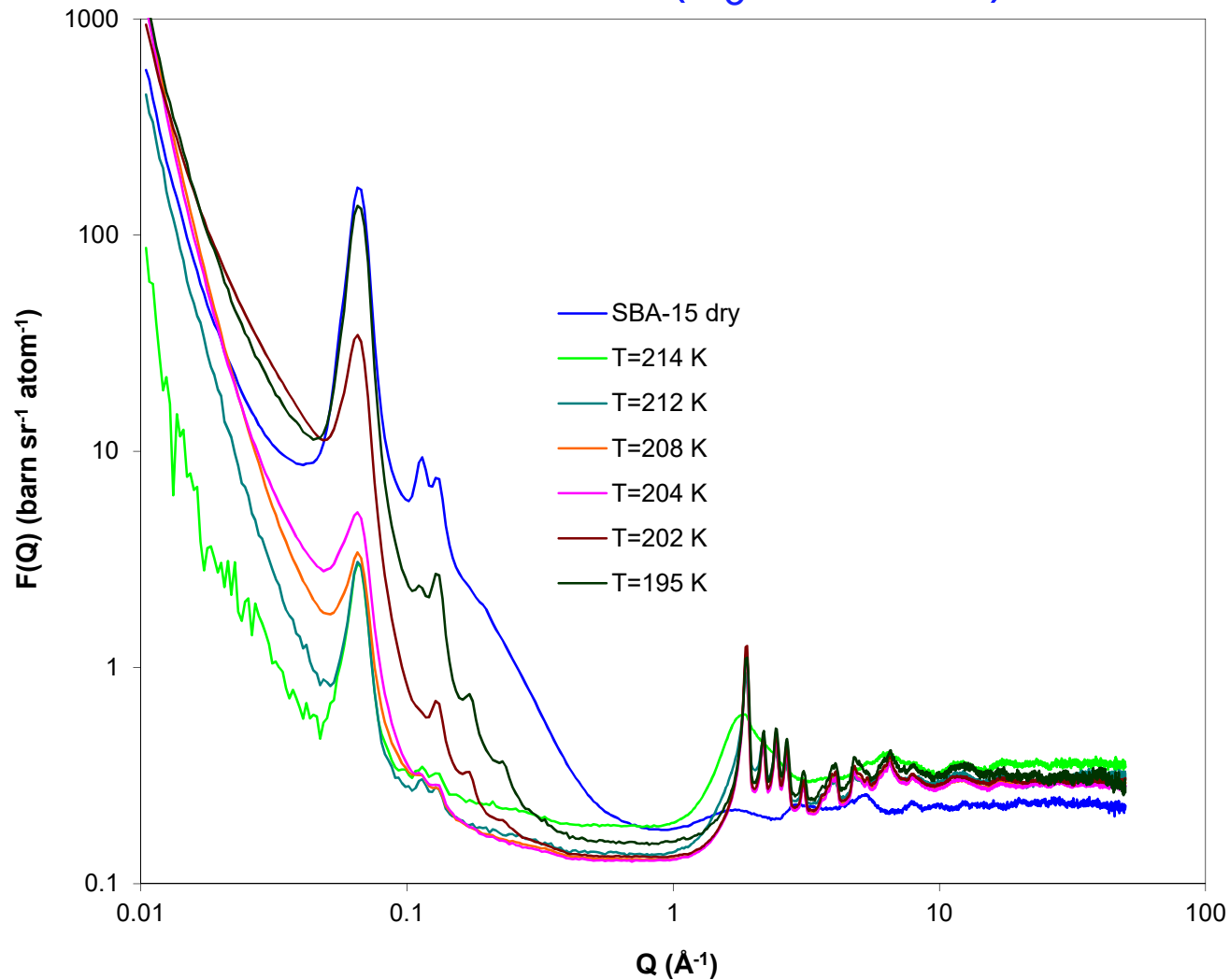




Total scattering structure factors and differential correlation functions for bulk liquid and confined CO_2

Cooling of confined CO₂ in SBA-15

$T=217 \rightarrow 195$ K ($T_3=216.6$ K)

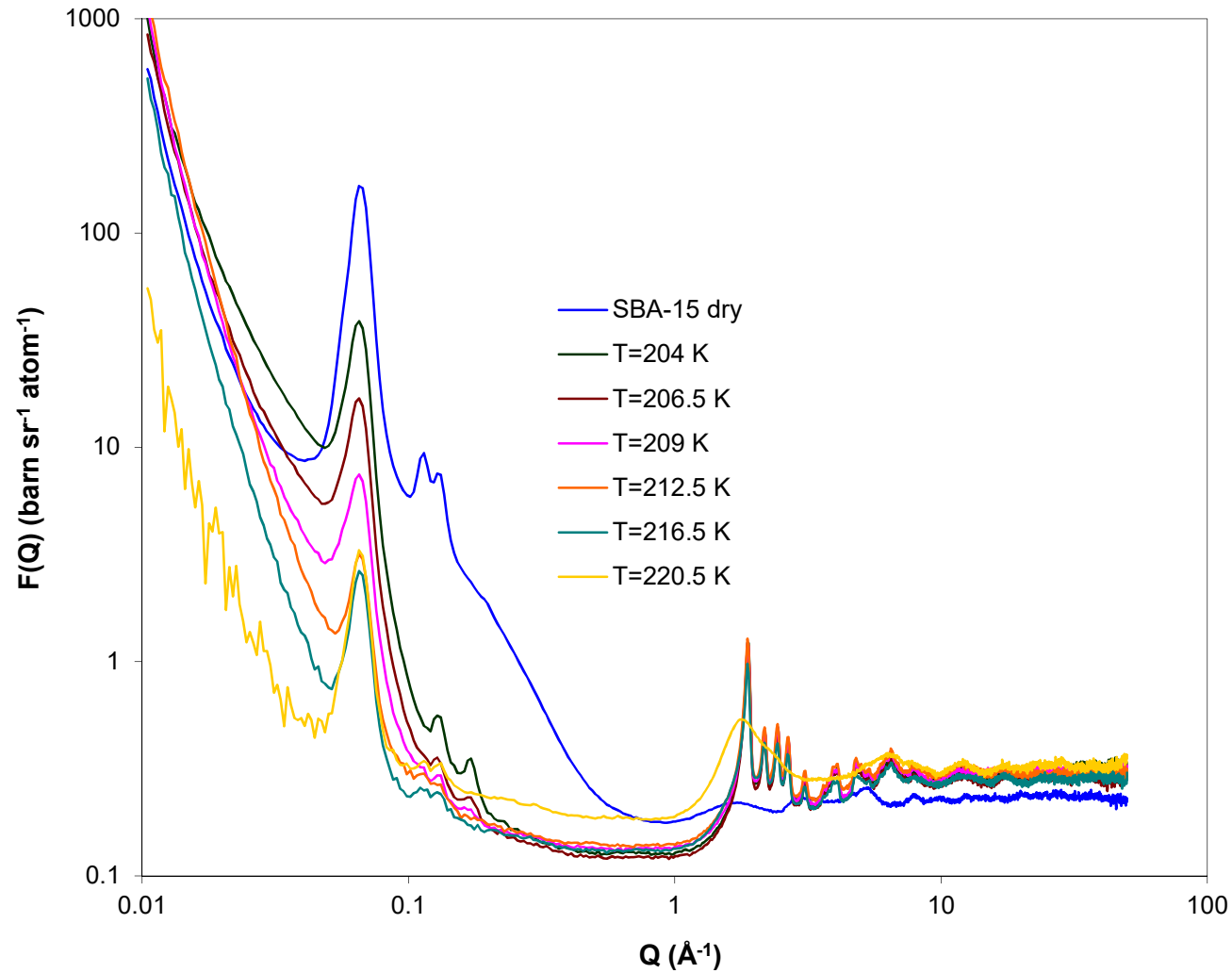


Differential scattering cross sections of CO₂ loaded SBA-15 (during cooling)

K.L. Stefanopoulos, F.K. Katsaros, Th.A. Steriotis, A.A. Sapalidis, M. Thommes, D.T. Bowron, T.G.A. Youngs, **Phys Rev. Lett.**, 116 (2016) 025502

Heating of confined CO₂ in SBA-15

$T=204 \rightarrow 220.5$ K ($T_3=216.6$ K)



Differential scattering cross sections of CO₂ loaded SBA-15 (during heating)

Summary

- **CO₂ adsorption with *in situ* neutron diffraction measurement on SBA-15 along an isotherm at $T=214$ K (NIMROD, ISIS).**
- **The structural properties of confined CO₂ just below the bulk triple point have liquid-like properties.**
- **Upon cooling below the bulk critical point, confined CO₂ molecules neither freeze nor remain liquid as expected, but escape from the pores. The process is reversible and during heating CO₂ refills the pores with temperature hysteresis.**

➤ **CO₂ confined in complex pore systems (limestone)**

Experiment

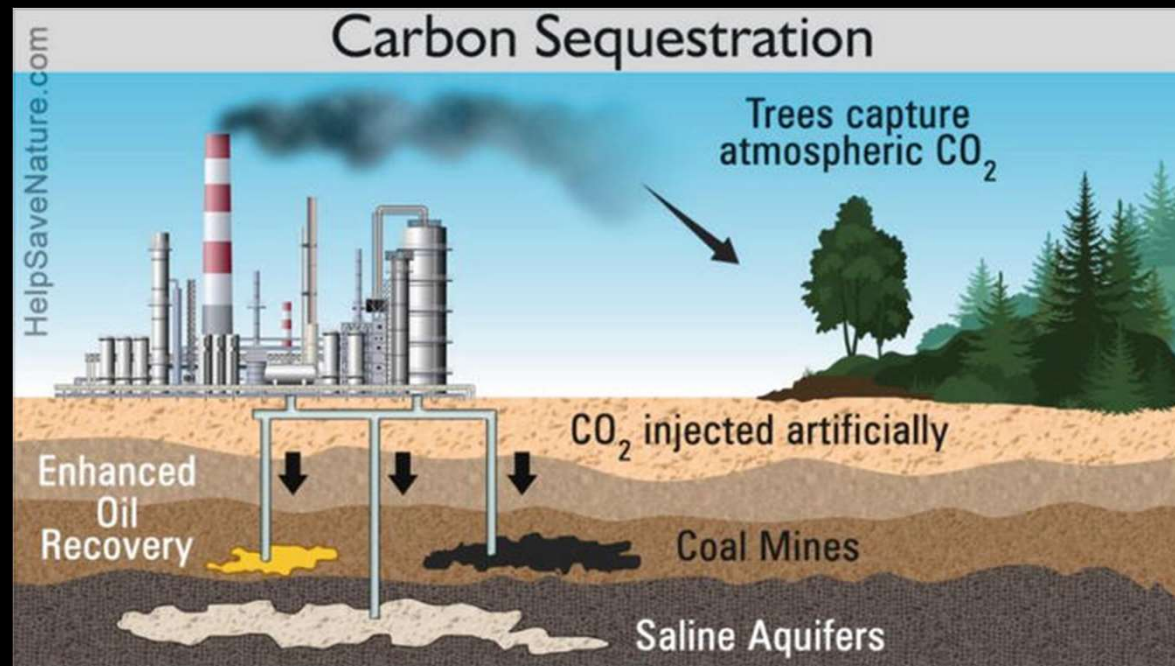
Performing in situ total neutron scattering measurements of supercritical CO₂ injected in empty and decane-loaded limestone samples

Goals of Study

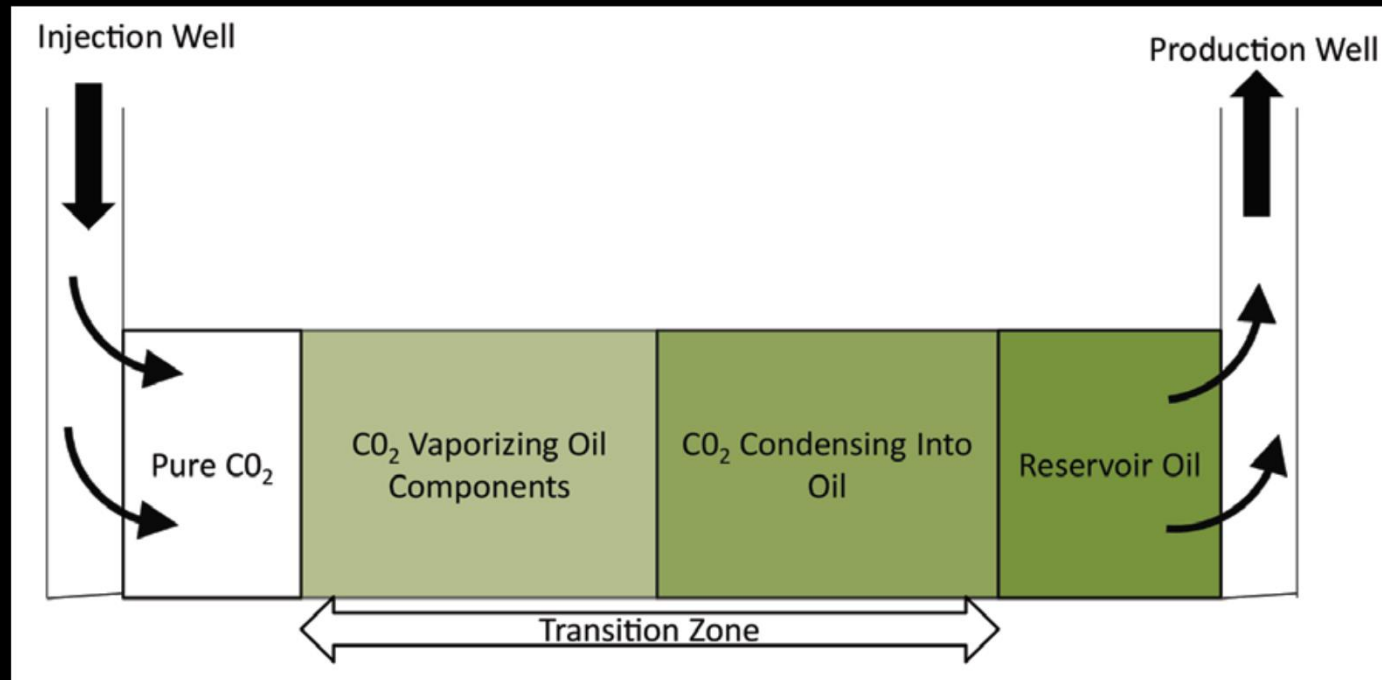
- Attempt to monitor the decane displacement upon supercritical CO₂ injection
- Attempt to calculate the fraction of pores inaccessible to CO₂
- Attempt to explore the structural properties of bulk and confined CO₂

Growing Role of CO₂-Enhanced Oil Recovery (CO₂-EOR)

- CO₂-EOR is applied as a tertiary recovery phase
- More than 50% of original-oil-in-place remains unrecovered after the primary and secondary phases of oil recovery
- CO₂-EOR currently provides the largest market demand for CO₂
- CO₂ may be safely sequestered in depleted oil and gas reservoirs



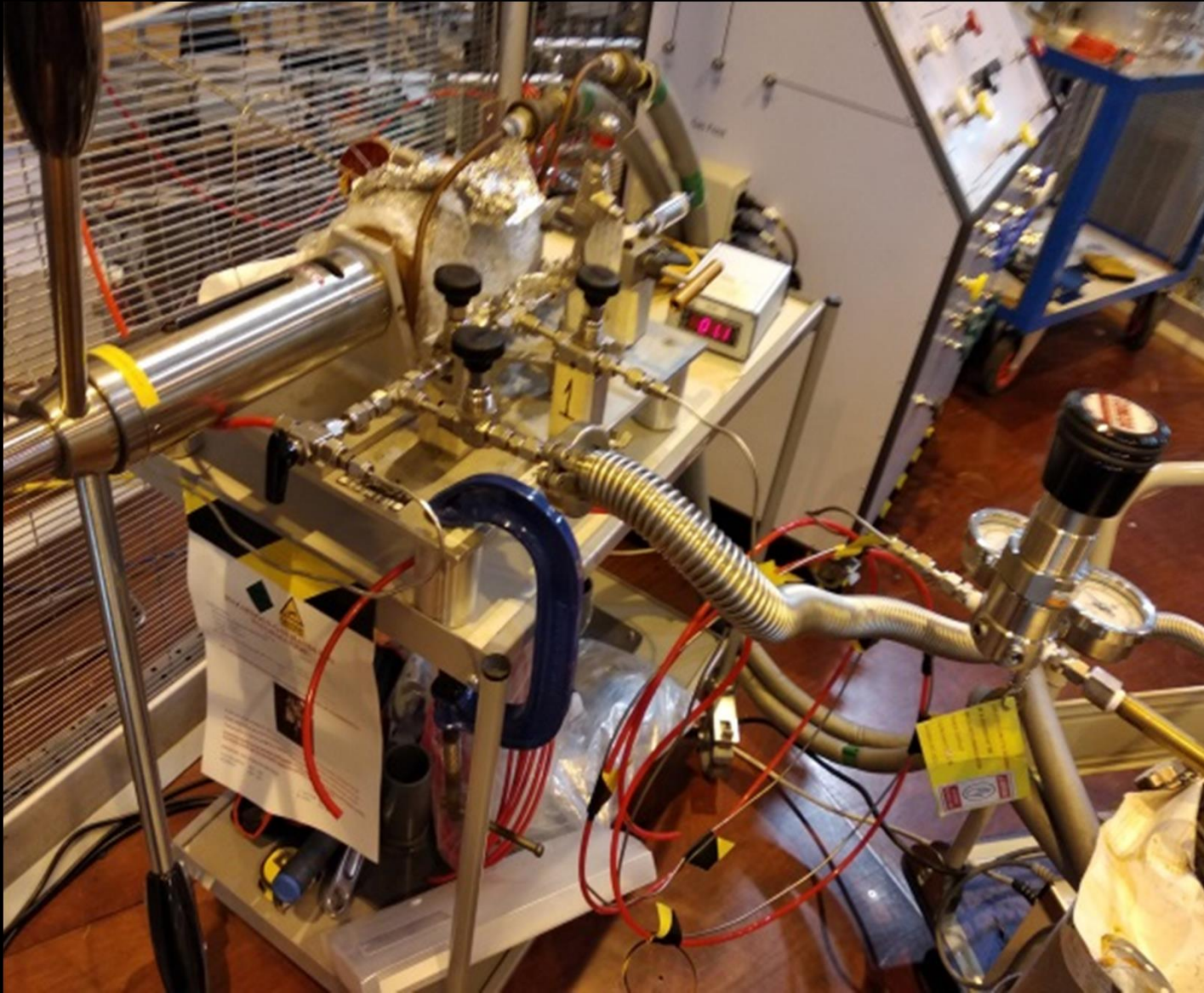
Schematic of CO₂-Enhanced Oil Recovery (CO₂-EOR)



Miscible CO₂-EOR process (pressures > MMP – higher recoveries)

- Higher molecular weight hydrocarbons vaporize into the CO₂
 - CO₂ dissolves in the oil causing oil swelling
 - Miscibility of the two phases is achieved
- A transition miscible zone is developed with the CO₂ in the back and the oil in the front

Experimental set-up

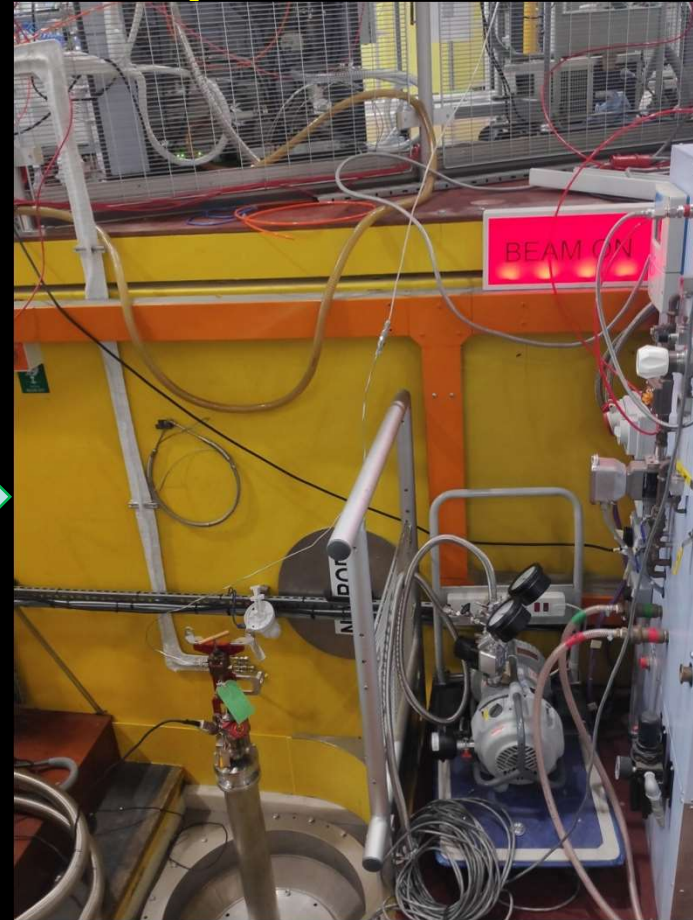


The gas handling apparatus connected with a CO₂ cylinder

Experimental set-up



The stick is connected to the gas handling apparatus and to the high-pressure cell



then placed in the neutron beam
under vacuum

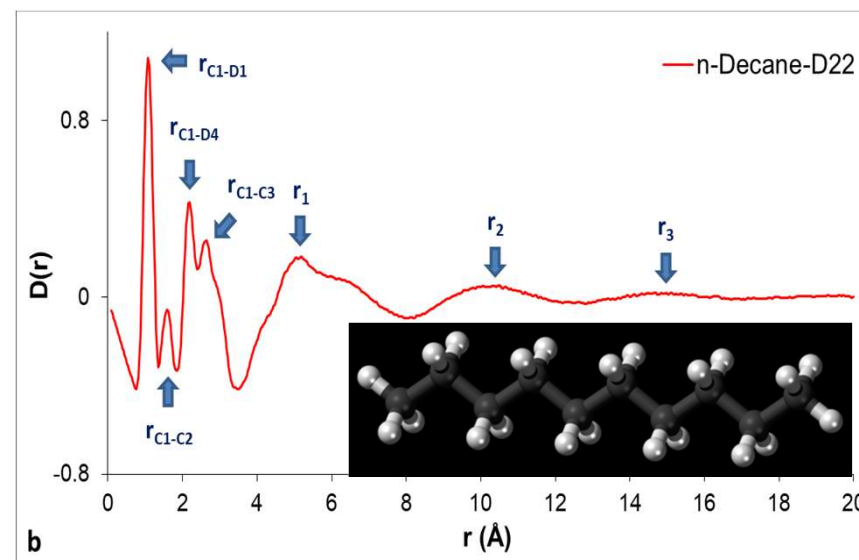
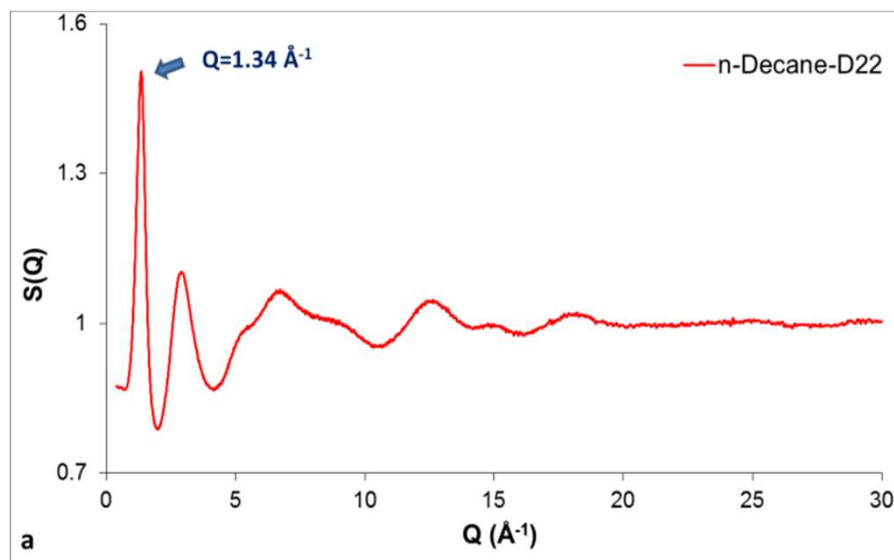
Experimental set-up



Samples were cut to fit the cell dimensions

High-pressure TiZr null coherent scattering cell (up to 1 kbar)

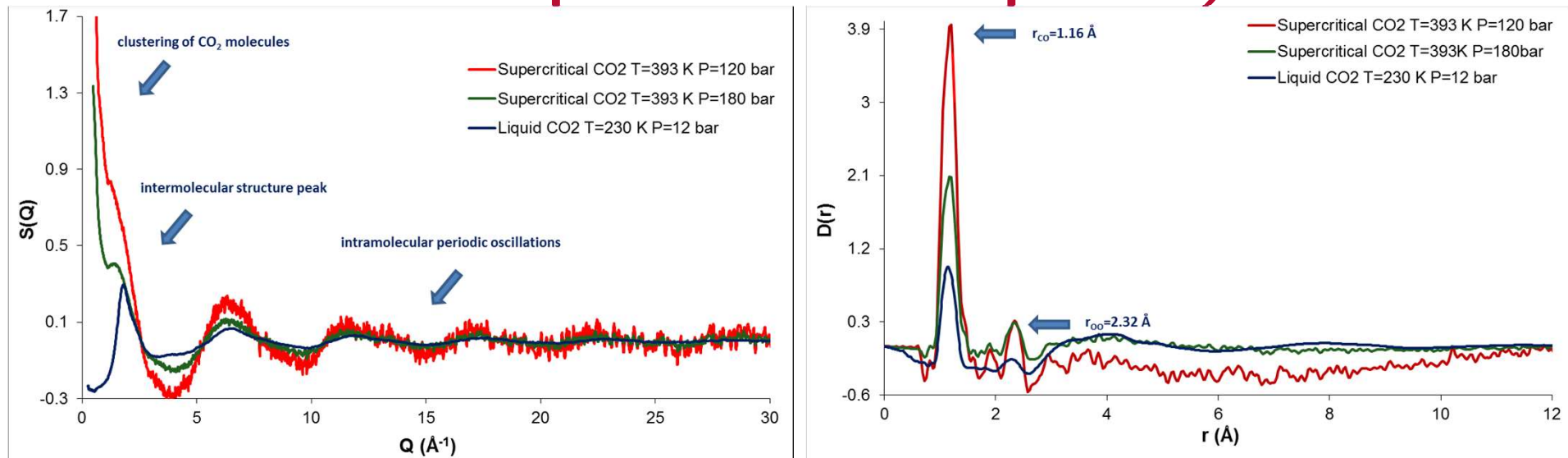
Bulk deuterated n-decane



(a) The total scattering structure factor and (b) the intra- and intermolecular part of differential correlation function for deuterated n-decane at 293 K and 1 atm.

| Correlation | Description | Symbol | Value |
|----------------|---|--------------------|-------|
| Intramolecular | Carbon-deuterium bond, C1-D1, etc. | $r_{\text{C1-D1}}$ | 1.08 |
| Intramolecular | Carbon-carbon bond, C1-C2 etc. | $r_{\text{C1-C2}}$ | 1.59 |
| Intramolecular | Carbon-deuterium on next carbon, C1-D4 etc. | $r_{\text{C1-D4}}$ | 2.16 |
| Intramolecular | Carbon-next but one carbon, C1-C3 etc. | $r_{\text{C1-C3}}$ | 2.64 |
| Intermolecular | Position of first-neighbour maximum | r_1 | 5.04 |
| Intermolecular | Position of second-neighbour maximum | r_2 | 10.47 |
| Intermolecular | Position of third-neighbour maximum | r_3 | 14.97 |

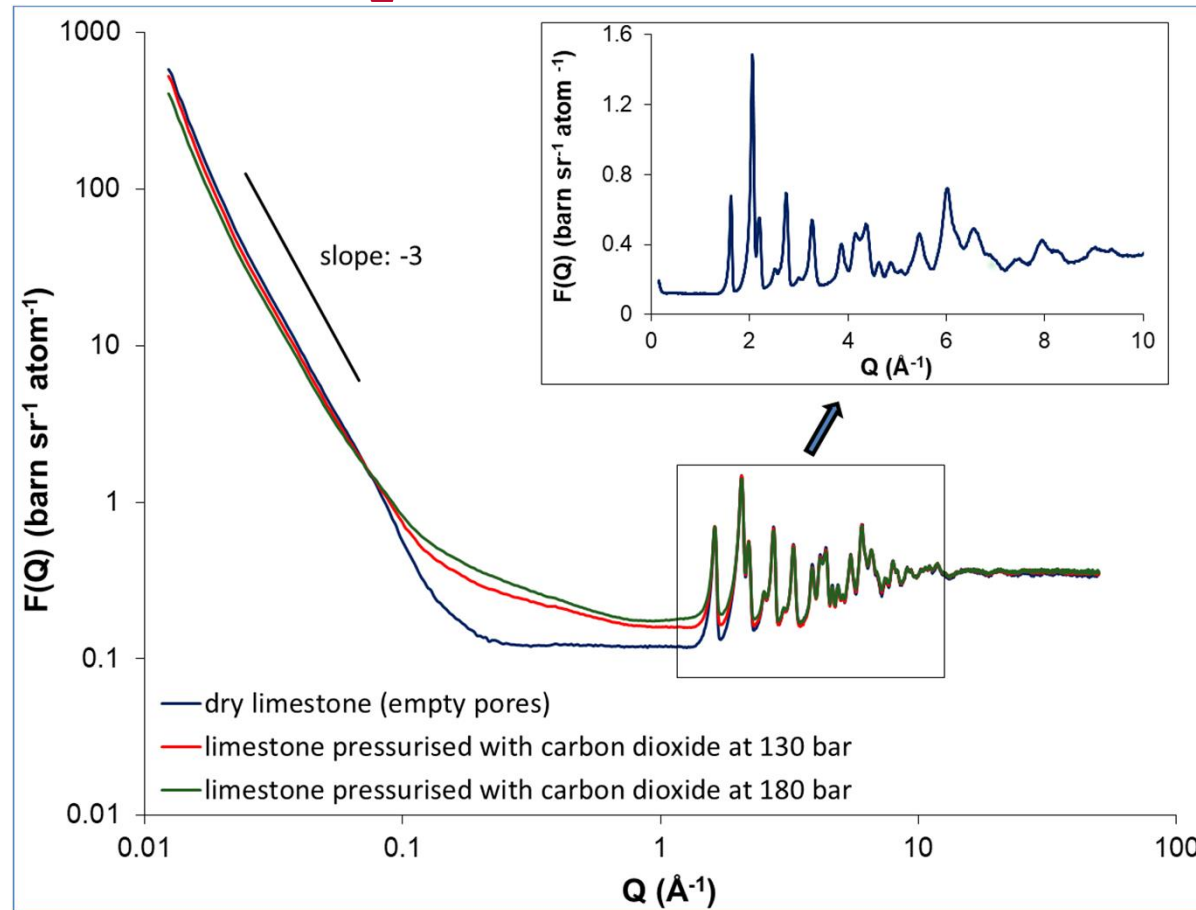
Bulk supercritical and liquid CO₂



The total scattering structure factor and the differential correlation function for bulk liquid and supercritical CO₂

- Strong scattering signal at low Q s from supercritical carbon dioxide suggests **clustering of CO₂ molecules** due to density fluctuations
- The intermolecular structure peak position is **density dependent**

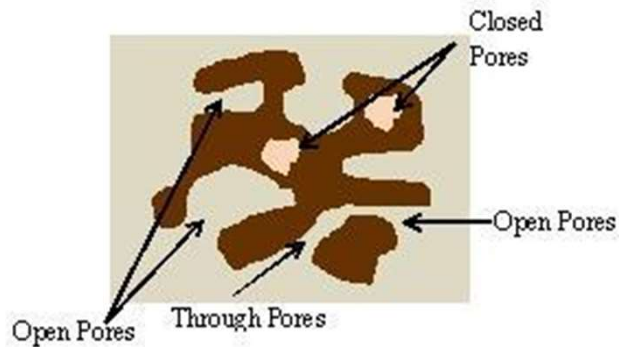
Supercritical CO₂ injection in empty limestone



- Upon pressurising with CO₂ the contrast at low Q ($Q < 0.08$ Å⁻¹) is reduced due to **pore filling**
- The slope at low Q (3.2) suggests a **fractally rough pore-rock interface***
- The intensity increase at high Q s mainly caused by **density fluctuations in supercritical CO₂**
- The **Bragg reflections from limestone** are clearly visible

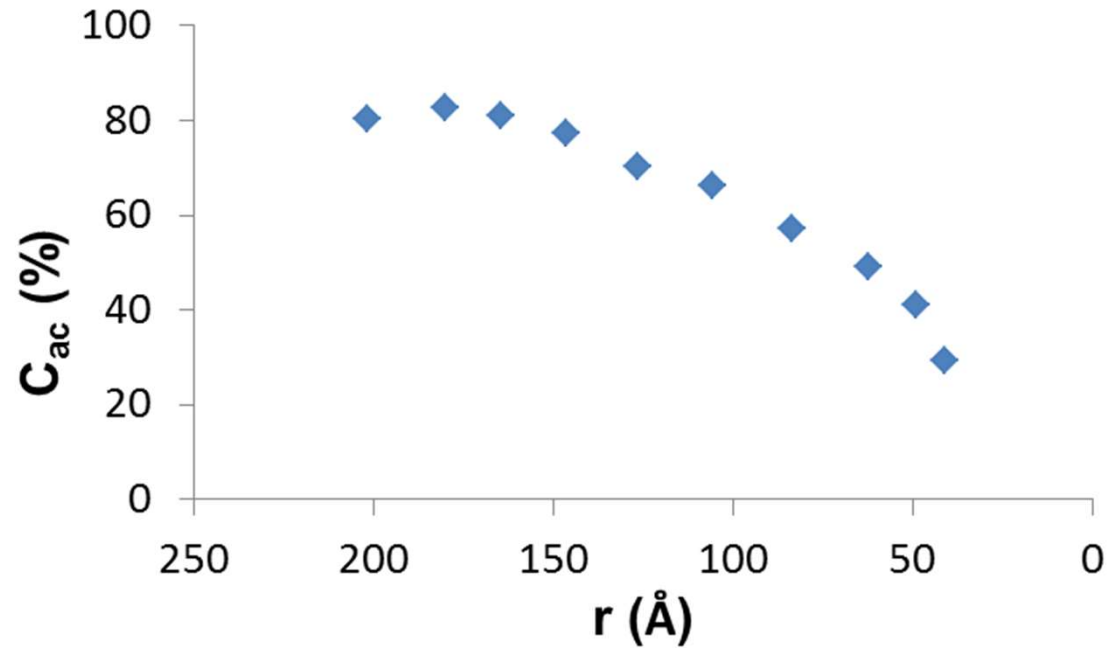
*K.L. Stefanopoulos, T.G.A. Youngs, R. Sakurovs, L.F. Ruppert, J. Bahadur, Y.B. Melnichenko, *Environm. Sci. Technol.*, 51 (2017) 6515

Pore accessibility to CO₂



$$\frac{I(P)}{I(0)} = S(P)C_{ac} + C_{in}$$

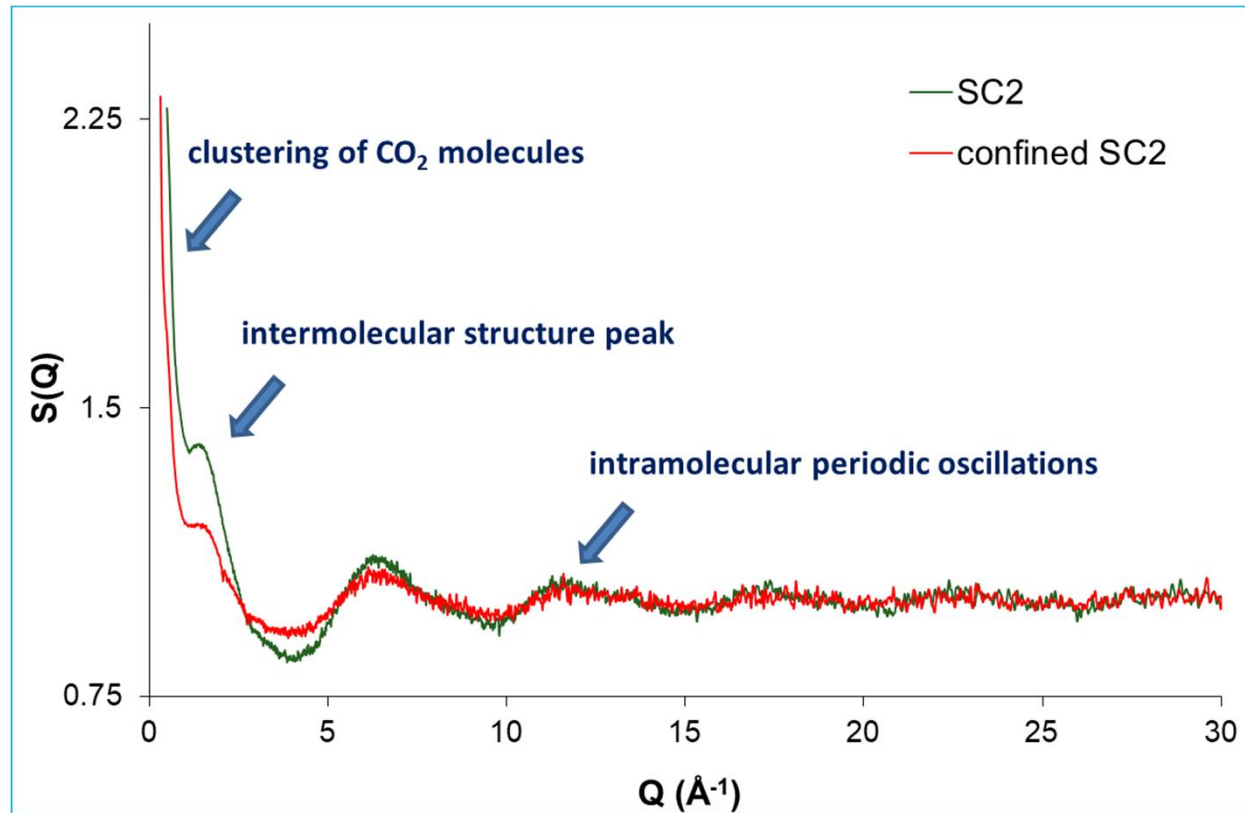
$$S(P) = \left[1 - \frac{\rho_f(P)}{\rho_m} \right]^2$$



The calculated volume fraction of accessible pores as a function of pore radius

➤ CO₂ is more accessible to large mesopores compared to small mesopores

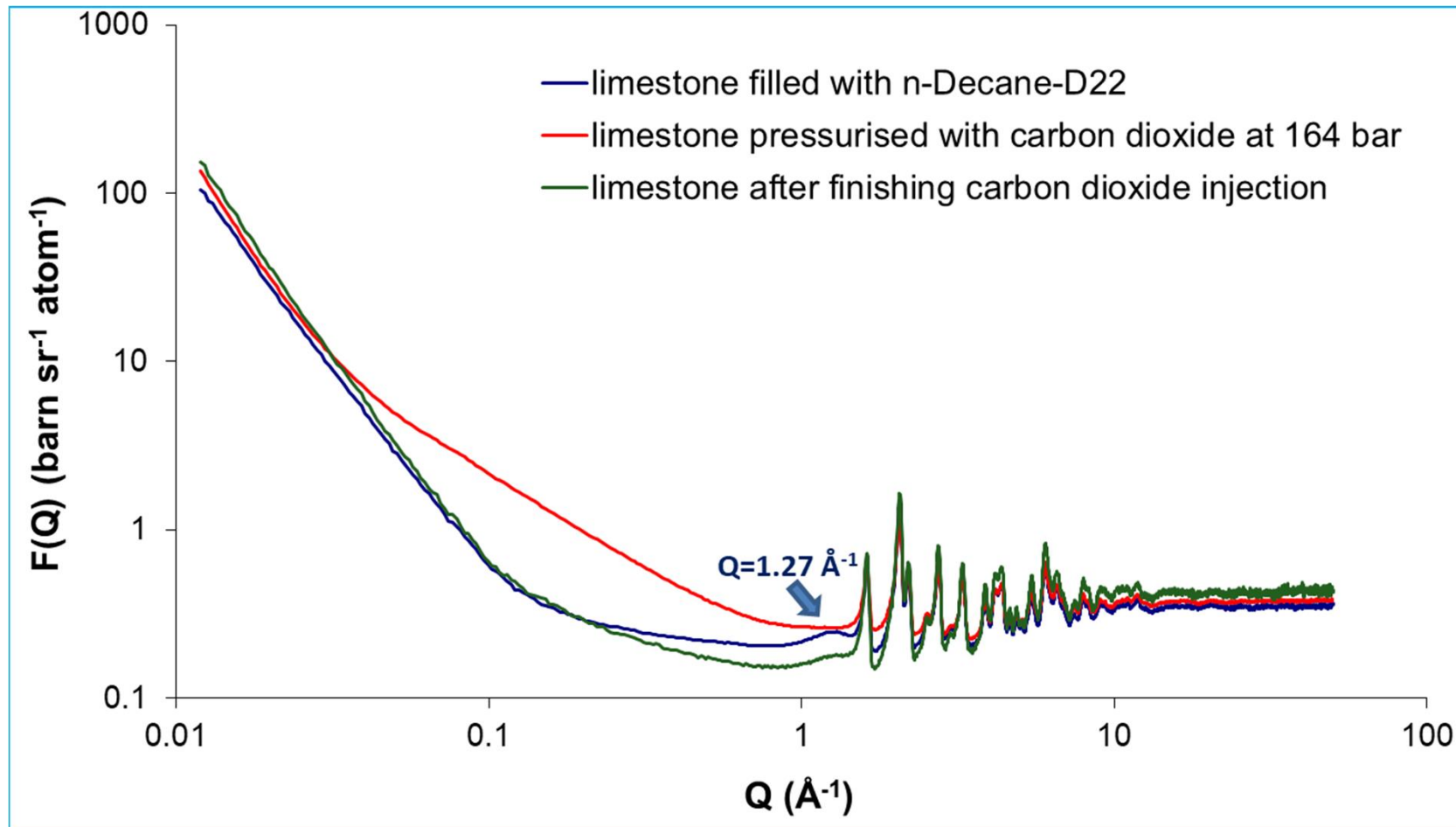
Bulk and confined supercritical CO₂



Total scattering structure factors for bulk (SC2) and confined supercritical CO₂ (confined SC2) at 393 K and 180 bar

- Strong SANS signal from bulk and confined CO₂
- Peak broadening and slight shift of the main structure peak to higher Q s for the confined CO₂ suggesting an increased density due to confinement

Supercritical CO₂ injection in limestone filled with decane



- Decane displacement after finishing CO₂ injection – decrease in the peak, contrast increase at low Q s
- There is still a remaining decane amount

Summary

- Monitoring the decane displacement at the nanoscale by *in situ* total neutron scattering.
- There was still a significant remaining decane amount possibly entrapped over the matrix surfaces and through the pore throats.
- Only a small fraction of the smaller mesopores is accessible to CO₂ suggesting that this class of pores is an unlikely site for underground CO₂ sequestration.
- Clustering of confined supercritical CO₂ molecules is also observed.

Team

Theodore Steriotis, Evangelos Favvas, Fotis Katsaros, Andreas Sapalidis, Vangelis Kouvelos, Chris Tampaxis, Nick Kanellopoulos

(NCSR Demokritos, Greece)

Tristan Youngs, Daniel Bowron, Tom Headen, Alex Hannon

(ISIS Neutron Source, STFC Rutherford, UK)

Yuri Melnichenko

(Oak Ridge National Laboratory-ORNL, USA)

George Karanikolos, Waleed Alameri, Vassilios Kelessidis

(Khalifa University of Science and Technology, Abu Dhabi, UAE)

Andreas Hoser

(Helmholtz Zentrum Berlin, Germany)

Nassos Mitropoulos

(International Hellenic University, Greece)

Financial Support

European Commission under TMR, 6th, 7th Framework and Horizon 2020 Programmes

Thank you!!!!